

**Ab initio study of magnetic properties of complexes formed by an Fe impurity and an intrinsic interstitial defect in ZnO**A. Debernardi<sup>1</sup> and M. Fanciulli<sup>1,2</sup><sup>1</sup>*MDM National Laboratory, CNR-INFN, via Olivetti 2, I-20041, Agrate Brianza, Italy*<sup>2</sup>*Dipartimento di Scienza dei Materiali, Università degli Studi Milano-Bicocca, I-20125 Milano, Italy*

(Received 3 March 2011; revised manuscript received 19 May 2011; published 11 July 2011)

By density functional supercell calculations we computed the total energy and the magnetic properties of isolated complexes formed in wurtzite ZnO doped with diluted Fe impurities in the presence of interstitial atoms of Zn or O. Interstitial O occupies preferentially a site with octahedral symmetry with substitutional Fe in the first neighbor shell, thus forming the complex  $\text{Fe}_{\text{Zn}}\text{-I}_{\text{O}}$ . In contrast, the complex  $\text{Fe}_{\text{Zn}}\text{-I}_{\text{Zn}}$  is energetically disfavored with respect to the case where the two components are far apart. For oxygen-rich growth conditions, a significant population of complexes  $\text{Fe}_{\text{Zn}}\text{-I}_{\text{O}}$  is stable at (and above) room temperature, providing a key to understanding the room-temperature magnetism of this system. Interstitial oxygen, coupled with diluted Fe impurities, exhibit a density of states spin polarized at the Fermi energy.

DOI: [10.1103/PhysRevB.84.024415](https://doi.org/10.1103/PhysRevB.84.024415)

PACS number(s): 75.50.Pp, 31.15.A–, 85.75.–d, 71.55.Gs

**I. INTRODUCTION**

The possibility to build up artificial magnetic materials by doping with magnetic impurities at diluted concentration nonmagnetic semiconductors which are commonly used by microelectronic industry has driven increasing attention to the field of diluted magnetic semiconductors (DMSs). The main target is the design and realization of devices with novel functionalities determined by the electron spin rather than the electron charge as in conventional electronic devices. To be useful for the electronics industry, spin-electronic (or spintronic) devices must present an electron density at the Fermi level fully spin-polarized.<sup>1</sup> Further, a material to be employed in spintronic devices of commercial use must have magnetic properties stable at (and above) room temperature. In this contest, ZnO doped with transition metal impurities has attracted considerable interest due to the prediction of ferromagnetism at room temperature.<sup>2</sup> The room-temperature magnetic properties of this compound have been largely debated<sup>3–5</sup> due to several experimental works showing the presence<sup>6–12</sup> or the absence<sup>13–15</sup> of ferromagnetism at room temperature. Recently, the Mössbauer spectra of diluted <sup>57</sup>Fe have been interpreted on the basis of  $\text{Fe}^{3+}$  paramagnet centers on substitutional Zn sites with unusually long relaxation times.<sup>16</sup> According to recent room-temperature photoluminescence experimental results on ZnO irradiated with high-energy electrons, the major acceptorlike defects were determined to be oxygen interstitials and zinc vacancies.<sup>17</sup>

In our previous work<sup>18</sup> we have computed the formation energy and the magnetic properties of isolated complexes formed by  $\text{Fe}_{\text{Zn}}$  with intrinsic vacancies, finding that ZnO doped with diluted Fe impurities can exhibit a room-temperature concentration of complexes involving Zn vacancies that considerably influence the magnetic properties.

In the present paper, we complete the theoretical investigation presented in Refs. 18–20 by studying the formation energy of isolated complexes formed by interstitial oxygen  $\text{I}_{\text{O}}$  and by interstitial zinc  $\text{I}_{\text{Zn}}$  in Fe-doped ZnO.

**II. COMPUTATIONAL DETAILS**

Our simulations are obtained by plane-wave pseudopotential techniques with spin-dependent density functional theory and with generalized gradient approximation of Perdew, Burke, and Ernzerhof (PBE)<sup>21</sup> as implemented in the PWSCF package (plane-wave self-consistent field).<sup>22</sup> We use state-of-the-art ultrasoft<sup>23,24</sup> pseudopotential in the separable form introduced by Kleinmann and Bylander.<sup>25</sup> O pseudopotential has 6 valence electrons, while the Zn one has 12 valence electrons. We compute the formation energy by using a  $3 \times 3 \times 2$  supercell (72 atoms for isolated  $\text{Fe}_{\text{Zn}}$  without vacancies) and relax atoms surrounding the defect within a radius of 3.95 Å in order to improve the convergence of the total energy with respect to the supercell size, according to the procedure adopted in Ref. 26 to study intrinsic defects in ZnO. The supercell lattice parameters are fixed to the bulk ones:  $a = 3.28$  Å,  $c = 5.30$  Å, obtained with the condition of vanishing stress and internal forces. The valence electronic density was expanded on a plane-wave basis set with a kinetic energy cutoff of 35 Ry, while for the augmentation density of ultrasoft pseudopotentials a cutoff of 560 Ry was used. Integration of electronic states is performed by means of special point techniques, by using (if not differently specified) a one-point Monkhorst-Pack<sup>27</sup> grid for the supercell and by means of smearing techniques in a similar way as done in Ref. 18.

For the charged defect, we computed the correction of repeated charges due to periodic boundary conditions according to the Leslie-Gillan method.<sup>28</sup> According to our calculation, the dielectric constant of the bulk system is almost isotropic: The component along  $c$  is  $\epsilon = 4.89$  and the component along  $a$  is  $\epsilon = 4.82$ ; that is, the difference between the two components is less than 2%. For this reason we take the average value ( $\epsilon_{\text{aver.}} = 4.84$ , considering the three Cartesian directions) when we compute the Leslie-Gillan correction.

**III. THEORY**

The defect concentration and the more stable configuration of complexes such as  $\text{Fe}_{\text{Zn}}\text{-I}_{\text{Zn}}$  ( $\text{I}_{\text{O}}$ ) is determined by the

formation energy,<sup>26</sup> which for a (neutral) charged defect reads

$$\Delta E_f = E(N_{\text{Zn}}, N_{\text{O}}, N_{\text{Fe}}) - N_{\text{Zn}}\mu_{\text{Zn}} - N_{\text{O}}\mu_{\text{O}} - N_{\text{Fe}}\mu_{\text{Fe}} + qE_F, \quad (1)$$

where  $E(N_{\text{Zn}}, N_{\text{O}}, N_{\text{Fe}})$  is the energy of the supercell containing  $N_{\text{Zn}}$  zinc,  $N_{\text{O}}$  oxygen, and  $N_{\text{Fe}}$  iron atoms;  $\mu_{\alpha}$  is the chemical potential of the  $\alpha$  element ( $\alpha = \text{Zn}, \text{O}, \text{Fe}$ );  $q$  is the charge of the defect (including its sign); and  $E_F$  is the Fermi energy. We conventionally take  $E_F$  to be zero at the top of the valence band and assume that its value can vary from the valence band edge up to the conduction band. Since, as usual in local density approximation, the fundamental band gap is underestimated ( $E_g = 0.745$  eV according to our simulation), we take the experimental band gap of  $E_g = 3.4$  eV for the energy range of  $E_F$  in a similar way as done in Ref. 29.

## IV. RESULTS

### A. Isolated intrinsic defects

Interstitial atoms in the wurtzite structure have two nonequivalent sites corresponding to two local minima of the energy: In one site the interstitial atom experiences a tetrahedral (tetra) symmetry; in the other site it experiences octahedral (octa) symmetry. For bulk ZnO, we found that the octahedral site is energetically favored with respect to the tetrahedral one for both  $I_{\text{O}}$  and  $I_{\text{Zn}}$  defects. The O atom in the octahedral site has an energy that is  $-0.362$  eV lower than the energy of O in the tetrahedral site, while for the Zn atom the octahedral site has an energy that is  $-1.999$  eV lower than the energy of Zn in the tetrahedral site. According to our results, the Zn interstitial,  $I_{\text{Zn}}$  is not a magnetic defect; at variance, the interstitial oxygen,  $I_{\text{O}}$ , has a magnetic moment of  $2.00\mu_B$  and  $0.26\mu_B$  for the octahedral and tetragonal sites, respectively.

### B. Neutral complexes

In Fig. 1 we display our results for the formation energy of the complexes  $\text{Fe}_{\text{Zn}}\text{-}I_{\text{O}}$  and  $\text{Fe}_{\text{Zn}}\text{-}I_{\text{Zn}}$ , as a function of Zn chemical potential. The lower values of  $\mu_{\text{Zn}}$  corresponds to O-rich (or equivalently Zn-poor) growth conditions, the higher values to O-poor (Zn-rich) conditions.

We have considered the complexes in which the  $\text{Fe}_{\text{Zn}}$  is in the nearest-neighbor shell with respect to the interstitial atom, giving two nonequivalent configurations for each interstitial site (octahedral or tetrahedra) considered. The formation energy of the configuration in which  $\text{Fe}_{\text{Zn}}$  and the interstitial atoms are infinitely far apart is also displayed (as a dashed line for O interstitial and as a dotted line for Zn interstitial). The zero of the energy corresponds to the formation energy of isolated  $\text{Fe}_{\text{Zn}}$ .

For the complexes involving  $I_{\text{Zn}}$  the configuration in which the  $\text{Fe}_{\text{Zn}}$  and the  $I_{\text{Zn}}$  in the octahedral position are infinitely far apart is energetically favored with respects to the configurations in which the Fe is in a neighbor shell with respect to  $I_{\text{Zn}}$ .

At variance, the complexes  $\text{Fe}_{\text{Zn}}\text{-}I_{\text{O}}$  have formation energy that is lower than the situation at which the Fe and the

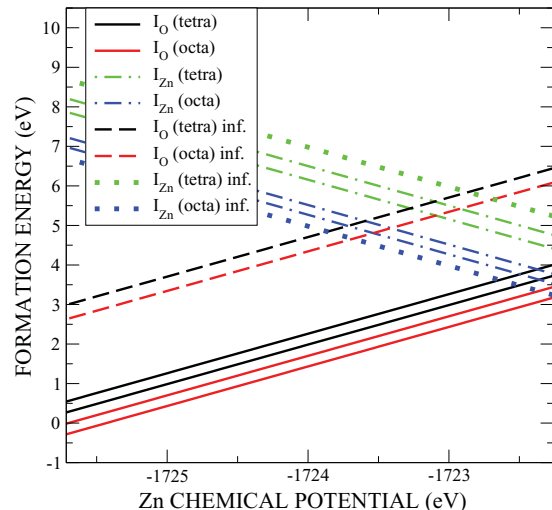


FIG. 1. (Color online) Formation energy of complexes  $\text{Fe}_{\text{Zn}}\text{-}I_{\text{O}}$  and  $\text{Fe}_{\text{Zn}}\text{-}I_{\text{Zn}}$  as a function of Zn chemical potential. The zero in the vertical axis corresponds to the formation energy of  $\text{Fe}_{\text{Zn}}$ .

interstitial O are far apart. In particular, as shown in Fig. 1, the complex  $\text{Fe}_{\text{Zn}}\text{-}I_{\text{O}}$  with the interstitial oxygen in the octahedral position is energetically favored with respect to the complexes in which  $I_{\text{O}}$  is tetrahedrally coordinated. Remarkably, for O-rich growth conditions (corresponding to the lower values of Zn chemical potential displayed in Fig. 1) the complex  $\text{Fe}_{\text{Zn}}\text{-}I_{\text{O}}$  (octa) has a formation energy that is comparable to the one of isolated Fe (the zero of the vertical scale in Fig. 1), allowing the formation of the complex  $\text{Fe}_{\text{Zn}}\text{-}I_{\text{O}}$  (octa) even at low temperature. For values of  $\mu_{\text{Zn}}$  slightly higher than the minimum of  $\mu_{\text{Zn}}$  in Fig. 1 the  $\Delta E_f$  of  $\text{Fe}_{\text{Zn}}\text{-}I_{\text{O}}$  (octa) or of  $\text{Fe}_{\text{Zn}}\text{-}I_{\text{O}}$  (tetra) are still a fraction of an electron volt, allowing the formation of a significant population of this complex at room temperature. This situation is similar to the one found in Ref. 18, where the complex  $\text{Fe}_{\text{Zn}}\text{-}V_{\text{Zn}}$  with  $V_{\text{Zn}}$  in the next-nearest-neighbor shell with respect to  $\text{Fe}_{\text{Zn}}$  is found to have negative formation energy for Zn-poor growth condition.

To deal with a quantity that can be directly compared to experimental data, we have computed the binding energy of the complex, defined as the difference between the formation energy of the system when the intrinsic defect is infinitely far apart from the substitutional iron and the formation energy of the complex. For the two nonequivalent complexes  $\text{Fe}_{\text{Zn}}\text{-}I_{\text{O}}$  (octa) investigated we computed a binding energy 2.9 and 2.6 eV. For the two nonequivalent complexes  $\text{Fe}_{\text{Zn}}\text{-}I_{\text{O}}$  (tetra) investigated we computed a binding energy 2.7 and 2.4 eV; in the latter complex the  $I_{\text{O}}$  is placed, with respect to the  $\text{Fe}_{\text{Zn}}$ , along the direction determined by  $c$  lattice parameter of the wurtzite structure.

In Fig. 2 and Fig. 3 we display the relaxed structure of the complex  $\text{Fe}_{\text{Zn}}\text{-}I_{\text{O}}$  (octa) with lowest formation energy. The spin-density isosurfaces ( $\pm 0.01\mu_B$ ) for majority and minority spin are also displayed in the same figures. From the figure one can notice the ferromagnetic coupling between the Fe and the interstitial O, while a small anti-ferro-magnetic coupling (minority spin) along the direction joining the  $\text{Fe}_{\text{Zn}}$  and the  $I_{\text{O}}$ . The total (absolute) magnetization per unit cell is  $3.80\mu_B$

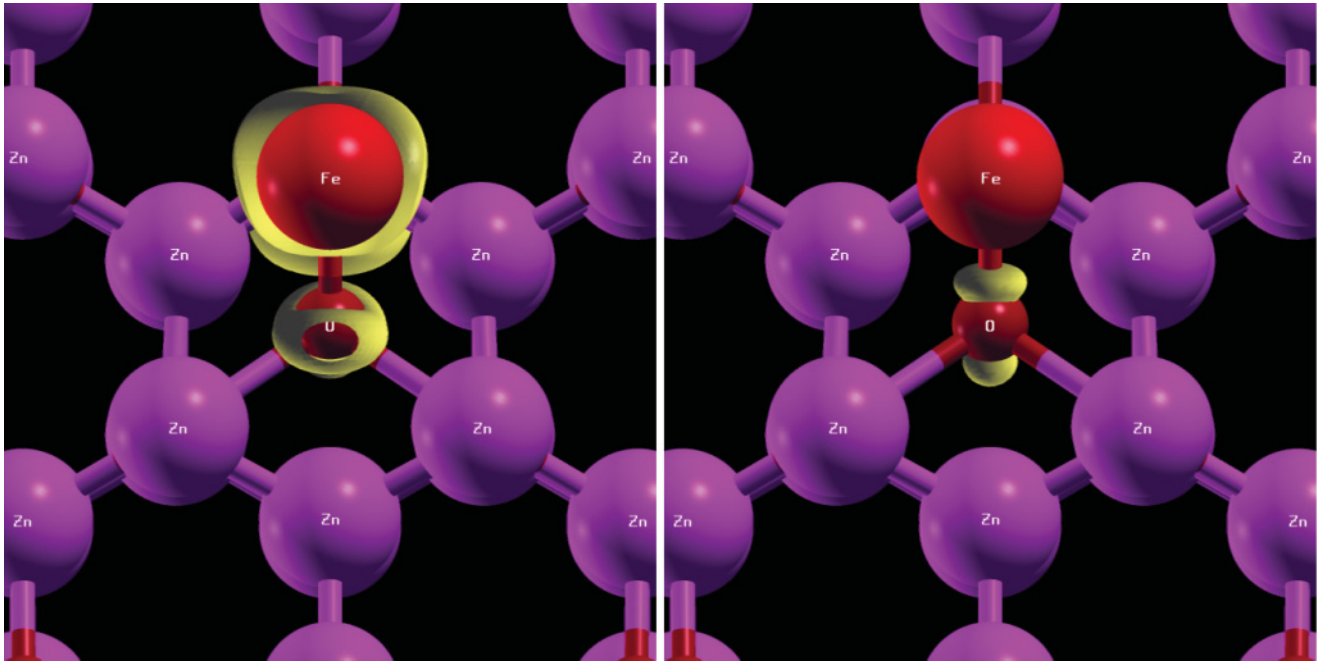


FIG. 2. (Color online) Top view of the complex  $\text{Fe}_{\text{Zn}}\text{-I}_O$  (octahedral site). In yellow are the isosurfaces for positive (0.01 a.u., left) and negative ( $-0.01$  a.u., right) spin density.

( $4.05 \mu_B$ ) while the total (absolute) magnetization of the other complex studied involving  $\text{I}_O$  at octahedral site is  $4.03 \mu_B$  ( $4.18 \mu_B$ )

In Fig. 4 we display the spin-resolved density of state (SDOS) of the complex  $\text{Fe}_{\text{Zn}}\text{-I}_O$  (octa) that presents the lowest energy among those investigated. The Fermi energy is almost superimposed to the valence band maximum of the minority spin, while the band edge of the majority spin is approximately

a fraction of an eV higher than  $E_F$ . The possibility that this complex can act as an acceptor is discussed in Sec. IV C.

In Fig. 5 we display the equilibrium configuration of the complex  $\text{Fe}_{\text{Zn}}\text{-I}_O$  (tetra) with lowest formation energy among the different configurations considered. The spin density isosurfaces ( $\pm 0.01 \mu_B$ ) for majority and minority spin are also displayed in the same figures. The total (absolute) magnetization per unit cell is  $3.88 \mu_B$  ( $4.05 \mu_B$ ), while the

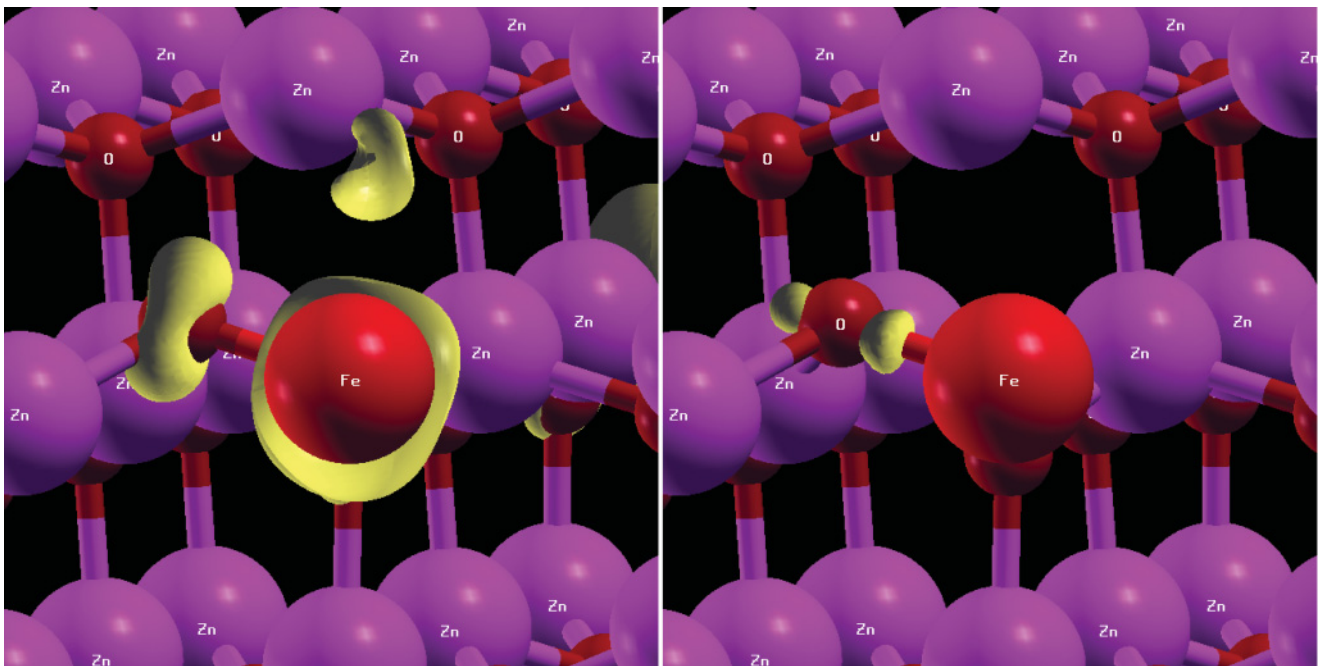


FIG. 3. (Color online) Side view of the complex  $\text{Fe}_{\text{Zn}}\text{-I}_O$  (octahedral site). In yellow are the isosurfaces for positive (0.01 a.u., left) and negative ( $-0.01$  a.u., right) spin density.

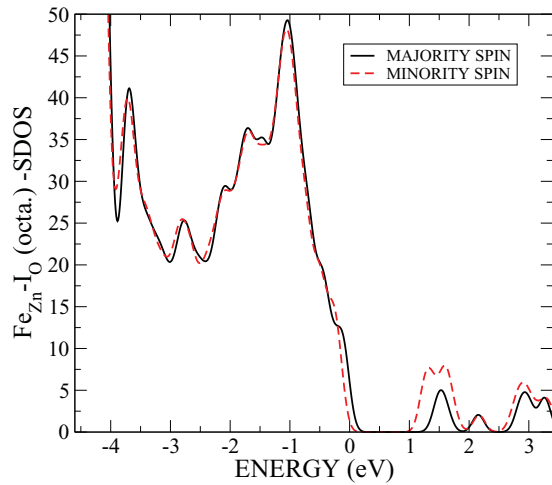


FIG. 4. (Color online) Density of state of majority and minority spin (SDOS) of ZnO with a complex formed by a substitutional Fe and an interstitial O at the octahedral site. The zero of the energy (horizontal scale) denotes the Fermi energy.

total magnetization of the other tetrahedral type complex (not displayed) is  $4.00\mu_B$  ( $4.40\mu_B$ ). From Fig. 5 one can notice the ferromagnetic coupling between the Fe and the interstitial O, as well as the O surrounding the  $\text{Fe}_{\text{Zn}}$ .

In Fig. 6 we display the SDOS corresponding to the complex  $\text{Fe}_{\text{Zn}}\text{-I}_\text{O}$  (tetra) displayed in Fig. 5. The Fermi energy is almost superimposed to the valence band maximum of the minority spin, while the band edge of the majority spin is approximately a fraction of eV higher than  $E_F$ , the possibility that this complex can act as an acceptor is discussed in Sec. IV C.

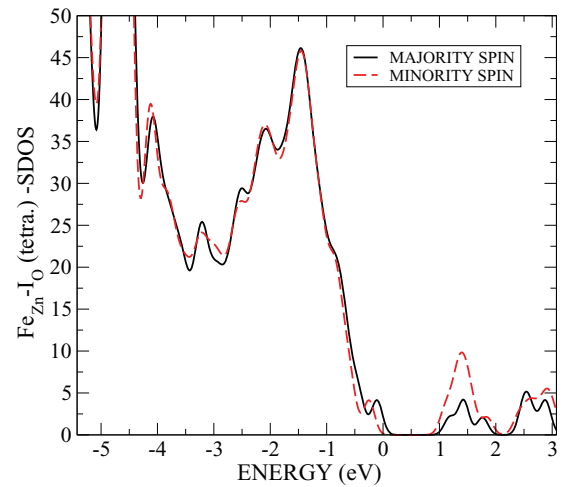


FIG. 6. (Color online) Density of state of majority and minority spin (SDOS) of ZnO doped with Fe impurity with interstitial O at the tetrahedral site. The zero of the energy (horizontal scale) denotes the Fermi energy.

We notice that the binding energy of the complexes  $\text{Fe}_{\text{Zn}}\text{-I}_\text{O}$  ranging from about 2.4 eV to about 2.9 eV (according the different configuration investigated) are considerably higher than the ones of  $\text{Fe}_{\text{Zn}}\text{-V}_{\text{Zn}}$  complexes,<sup>18</sup> which are  $\sim 1.4, 1.7$  eV for  $\text{V}_{\text{Zn}}$  in the fourth and in the next-nearest-neighbor shell to  $\text{Fe}_{\text{Zn}}$ , respectively. According to the suggestion of Ref. 18 the  $\text{Fe}_{\text{Zn}}\text{-V}_{\text{Zn}}$  complexes can be associated with two different complexes involving Zn vacancies that are annealed out at 400 K and 550 K.<sup>30</sup> Due to the larger binding energy of the complexes  $\text{Fe}_{\text{Zn}}\text{-I}_\text{O}$ , we expect these defects to be stable up to very high temperature.

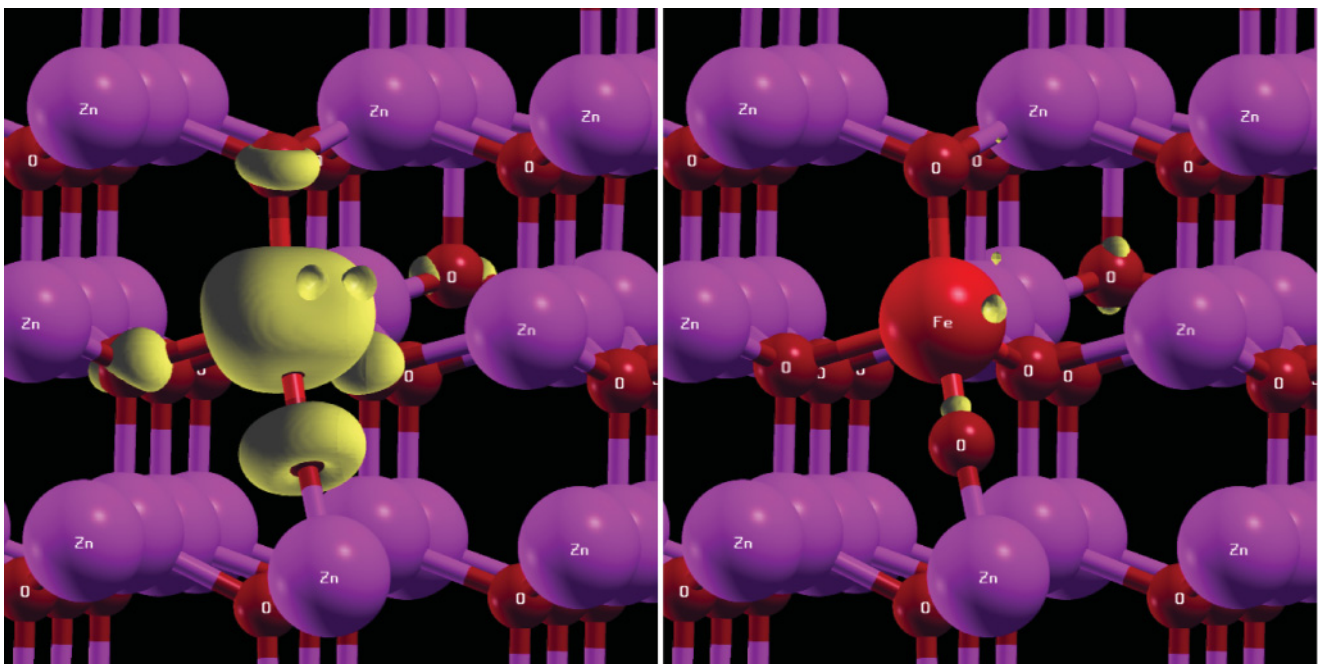


FIG. 5. (Color online) Side view of the complex  $\text{Fe}_{\text{Zn}}\text{-I}_\text{O}$  (tetrahedral site). In yellow are the isosurfaces for positive (0.01 a.u., left) and negative ( $-0.01$  a.u., right) spin density.

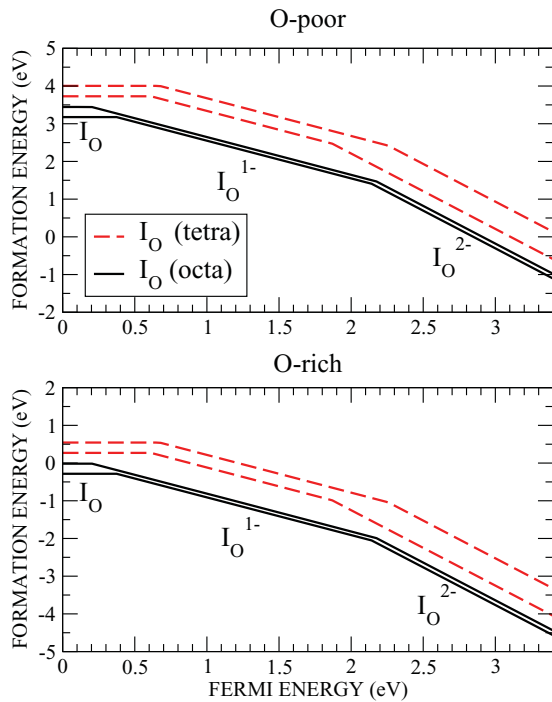


FIG. 7. (Color online) Formation energy of neutral and charged complexes  $\text{Fe}_{\text{Zn}}\text{-I}_{\text{O}}$  as a function of Fermi energy for O-poor (top) and O-rich (bottom) growth conditions. For each  $\text{Fe}_{\text{Zn}}\text{-I}_{\text{O}}$  configuration only the (charged/neutral) defect with lower energy is displayed. The zero in the vertical axis corresponds to the formation energy of  $\text{Fe}_{\text{Zn}}$ .

### C. Charged complexes

According to the results displayed in Fig. 1, the complexes involving substitutional Fe and a Zn interstitial have formation energy larger than 3 eV; further, the complex with lower formation energy is the one in which  $\text{Fe}_{\text{Zn}}$  and  $\text{I}_{\text{Zn}}$  are far apart. For this reason, in studying the charged complexes, we consider only the complexes involving oxygen interstitial. In Fig. 7, we display the computed formation energy of neutral and charged complexes  $\text{Fe}_{\text{Zn}}\text{-I}_{\text{O}}$  as a function of the Fermi energy for O-poor (top panel) and O-rich (bottom panel) growth condition. In the same figure we also display the formation energy corresponding to the configuration in which  $\text{Fe}_{\text{Zn}}$  and  $\text{I}_{\text{O}}$  (tetra/octa) are far apart (in the calculation for non-neutral  $\text{I}_{\text{O}}$  far apart from the  $\text{Fe}_{\text{Zn}}$  we have assumed that the negative charge remains localized at the interstitial oxygen site). We computed the formation energy of the neutral and charged (with one and two electron added)  $\text{Fe}_{\text{Zn}}\text{-I}_{\text{O}}$  complex with the interstitial O at the octahedral and at the tetrahedral sites. For simplicity, in the figure for each complex involving O interstitial at tetrahedral or octahedral site, we display only the results for the complex (including the charged state) having the lowest formation energy. As can be noticed from the figure, the lines corresponding to the formation energies

of different complexes do not intersect; that is, the complex with  $\text{I}_{\text{O}}$  in the octahedral position remains the one with the lowest formation energy. From the figure, we notice that at about 0.4 eV the charged complex (1-) becomes stable. From these results and simple stoichiometric considerations, one can suggest that the this (1-) complex presents iron in a  $\text{Fe}^{3+}$  state and the complex acts as a acceptor.

As the Fermi energy increases the complex  $\text{Fe}_{\text{Zn}}\text{-I}_{\text{O}}$  (octa) accepts one or two electrons end the energy difference with the other complex investigated having  $\text{I}_{\text{O}}$  in the octahedral site reduces. Notably, in the case of O-rich conditions, for  $E_F$  close to the bottom of the conduction band the formation energy of doubly charged  $\text{Fe}_{\text{Zn}}\text{-I}_{\text{O}}$  (octa) complex is more than four electron volts lower than the one of isolated  $\text{Fe}_{\text{Zn}}$ . For  $E_F = 3.4$  eV (i.e., at the bottom of the conduction band) the binding energy of the  $\text{Fe}_{\text{Zn}}\text{-I}_{\text{O}}$  (octa) with lowest energy is 3.8 eV for O-poor and for O-rich growth conditions. The total (absolute) magnetic moments corresponding to the charged  $\text{Fe}_{\text{Zn}}\text{-I}_{\text{O}}$  (octa) having lowest energy among the complexes investigate are  $4.92\mu_B$  ( $4.97\mu_B$ ) for charged defect with one electron and  $4.97\mu_B$  ( $5.05\mu_B$ ) for charged defect with two electrons.<sup>31</sup>

### V. CONCLUSIONS

In summary, by *ab initio* calculations we investigated the magnetic properties of isolated complexes formed in wurtzite ZnO doped with diluted Fe impurities in presence of oxygen and zinc interstitials. Our study, combined with those of Ref. 18, provide a systematic investigation of the formation energy and magnetic properties of different type of complexes formed by  $\text{Fe}_{\text{Zn}}$  and an intrinsic defect ( $\text{V}_{\text{Zn}}$ ,  $\text{V}_{\text{O}}$ ,  $\text{I}_{\text{O}}$ ,  $\text{I}_{\text{Zn}}$ ) in wurtzite ZnO. We found that for Zn-poor growth conditions the formation of  $\text{Fe}_{\text{Zn}}\text{-I}_{\text{O}}$  complexes is energetically favored. A similar situation was found in Ref. 18 for the complex  $\text{Fe}_{\text{Zn}}\text{-V}_{\text{Zn}}$ . Remarkably these stable complexes are the ones formed by the magnetic impurity  $\text{Fe}_{\text{Zn}}$  with one of the two intrinsic defects of ZnO ( $\text{I}_{\text{O}}$  and  $\text{V}_{\text{Zn}}$ ) that present a spin polarization also when they are isolated, that is, far apart from other impurities. The present work suggests a possible key role of oxygen interstitial as well as of zinc vacancy<sup>18</sup> to enlighten the microscopic mechanisms responsible for the magnetism experimentally detected in ZnO:Fe at room temperature. The nature of the magnetic coupling between different complexes is not addressed in the present work and will be the object of future investigations.

### ACKNOWLEDGMENTS

Useful discussions with R. Sielemann and G. Langouche are gratefully acknowledged. We acknowledge computational resources provided under the “Iniziativa trasversale di calcolo parallelo” (2008–2010 CINECA grant).

<sup>1</sup>See, e.g., K. Sato, L. Bergqvist, J. Kudornovský, P. H. Dederichs, O. Eriksson, I. Turek, B. Sanyal, G. Bouzerar, H. Katayama-Yoshida, V. A. Dinh, T. Fukushima, H. Kizaki, and R. Zeller,

*Rev. Mod. Phys.* **82**, 1633 (2010); A. Zunger, S. Lany, and H. Reabiger, *Physics* **3**, 53 (2010); T. Dietl, *Net. Mater.* **9**, 965 (2010).

- <sup>2</sup>T. Dietl, H. Ohno, F. Matsukura, J. Cibert, and D. Ferrand, *Science* **287**, 1019 (2000).
- <sup>3</sup>B. B. Straumal, A. A. Mazilkin, S. G. Protasova, A. A. Myatiev, P. B. Straumal, G. Schutz, P. A. van Aken, E. Goering, and B. Baretzky, *Phys. Rev. B* **79**, 205206 (2009).
- <sup>4</sup>G. Weier, H. P. Gunnlaugsson, R. Mantovan, M. Fanciulli, D. Naidoo, K. Bharuth-Ram, and T. Agne, *J. Appl. Phys.* **102**, 113915 (2007).
- <sup>5</sup>D. Azamat and M. Fanciulli, *Physica B* **401**, 382 (2007).
- <sup>6</sup>M. Venkatesan, C. B. Fitzgerald, J. G. Lunney, and J. M. D. Coey, *Phys. Rev. Lett.* **93**, 177206 (2004).
- <sup>7</sup>P. Wu, G. Saraf, Y. Lu, D. H. Hill, R. Gateau, L. Wielunski, R. A. Bartynski, D. A. Arena, J. Dvorak, A. Moodenbaugh, T. Siegrist, J. A. Raley, and Y. K. Yeo, *Appl. Phys. Lett.* **89**, 012508 (2006).
- <sup>8</sup>C. Song, K. W. Geng, F. Zeng, X. B. Wang, Y. X. Shen, F. Pan, Y. N. Xie, T. Liu, H. T. Zhou, and Z. Fan, *Phys. Rev. B* **73**, 024405 (2006).
- <sup>9</sup>N. H. Hong, J. Sakai, N. T. Huong, N. Poirot, and A. Ruyter, *Phys. Rev. B* **72**, 045336 (2005).
- <sup>10</sup>K. R. Kittilstved, N. S. Norberg, and D. R. Gamelin, *Phys. Rev. Lett.* **94**, 147209 (2005).
- <sup>11</sup>Q. Wang, Q. Sun, P. Jena, and Y. Kawazoe, *Phys. Rev. B* **70**, 052408 (2004).
- <sup>12</sup>D. Karmakar, S. K. Mandal, R. M. Kadam, P. L. Paulose, A. K. Rajarajan, T. K. Nath, A. K. Das, I. Dasgupta, and G. P. Das, *Phys. Rev. B* **75**, 144404 (2007).
- <sup>13</sup>S. Kolesnik, B. Dabrowski, and J. Mais, *J. Appl. Phys.* **95**, 2582 (2004).
- <sup>14</sup>S. Kolesnik and B. Dabrowski, *J. Appl. Phys.* **96**, 5379 (2004).
- <sup>15</sup>G. Lawes, A. S. Risbud, A. P. Ramirez, and R. Seshadri, *Phys. Rev. B* **71**, 045201 (2005).
- <sup>16</sup>H. P. Gunnlaugsson, T. E. Mølholt, R. Mantovan, H. Masenda, D. Naidoo, W. B. Dlamini, R. Sielemann, K. Bharuth-Ram, G. Weyer, K. Johnston, G. Langouche, S. Ólafsson, H. P. Gíslason, Y. Kobayashi, Y. Yoshida, and M. Fanciulli, *Appl. Phys. Lett.* **97**, 142501 (2010).
- <sup>17</sup>E.-J. Yun, J. W. Jung, Y. H. Han, M.-W. Kim, and B. C. Lee, *J. Appl. Phys.* **105**, 123509 (2009).
- <sup>18</sup>A. Debernardi and M. Fanciulli, *Appl. Phys. Lett.* **90**, 212510 (2007).
- <sup>19</sup>A. Debernardi and M. Fanciulli, *Physica B* **401**, 451 (2007).
- <sup>20</sup>A. Debernardi and M. Fanciulli, *Physica B* **404**, 4791 (2009).
- <sup>21</sup>J. P. Perdew, K. Burke, and M. Ernzerhof, *Phys. Rev. Lett.* **77**, 3865 (1996); **78**, 1396(E) (1997).
- <sup>22</sup>S. Baroni, A. Dal Corso, S. de Gironcoli, and P. Giannozzi, [<http://www.pwscf.org>].
- <sup>23</sup>A. M. Rappe, K. M. Rabe, E. Kaxiras, and J. D. Joannopoulos, *Phys. Rev. B* **41**, 1227 (1990).
- <sup>24</sup>D. Vanderbilt, *Phys. Rev. B* **32**, 8412 (1985).
- <sup>25</sup>L. Kleinman and D. M. Bylander, *Phys. Rev. Lett.* **48**, 1425 (1982).
- <sup>26</sup>A. F. Kohan, G. Ceder, D. Morgan, and Chris G. Van de Walle, *Phys. Rev. B* **61**, 15019 (2000).
- <sup>27</sup>H. J. Monkhorst and J. D. Pack, *Phys. Rev. B* **13**, 5188 (1976).
- <sup>28</sup>M. Leslie and M. J. Gillan, *J. Phys. C* **18**, 973 (1985).
- <sup>29</sup>A. Jannotti and C. G. Van de Walle, *Appl. Phys. Lett.* **87**, 122102 (2005).
- <sup>30</sup>F. Tuomisto, K. Saarinen, D. C. Look, and G. C. Farlow, *Phys. Rev. B* **72**, 085206 (2005).
- <sup>31</sup>The magnetic moments are computed with a (222) MP grid to obtain a converged magnetization for the charged complexes. At variance, the qualitative behavior of the formation energies of neutral and charged complexes do not change by increasing the special points sampling to (222) MP grid.